Digital simulation of two-dimensional random fields with arbitrary power spectra and non-Gaussian probability distribution functions

Yura, Harold; Hanson, Steen Grüner

Published in:
Applied Optics

Link to article, DOI:
10.1364/AO.51.000C77

Publication date:
2012

Document Version
Publisher's PDF, also known as Version of record

Citation (APA):
Yura, H., & Hanson, S. G. (2012). Digital simulation of two-dimensional random fields with arbitrary power spectra and non-Gaussian probability distribution functions. *Applied Optics*, *51*(10), C77-C83. https://doi.org/10.1364/AO.51.000C77

Digital simulation of two-dimensional random fields with arbitrary power spectra and non-Gaussian probability distribution functions

Harold T. Yura[1] and Steen G. Hanson[2,*]

[1]Electronics and Photonics Laboratory, The Aerospace Corporation, Los Angeles, California 90009, USA

[2]DTU Fotonik, Department of Photonics Engineering, Danish Technical University, 4000 Roskilde, Denmark

*Corresponding author: Steen.Hanson@fotonik.dtu.dk

Received 19 December 2011; accepted 2 February 2012;
posted 7 February 2012 (Doc. ID 160058); published 23 March 2012

Methods for simulation of two-dimensional signals with arbitrary power spectral densities and signal amplitude probability density functions are disclosed. The method relies on initially transforming a white noise sample set of random Gaussian distributed numbers into a corresponding set with the desired spectral distribution, after which this colored Gaussian probability distribution is transformed via an inverse transform into the desired probability distribution. In most cases the method provides satisfactory results and can thus be considered an engineering approach. Several illustrative examples with relevance for optics are given. © 2012 Optical Society of America

OCIS codes: 030.1640, 120.7250, 030.1670, 030.6140, 030.6600.

1. Introduction

Optical sensing has been of uttermost importance for centuries and will gain increasingly more importance as the development of new optical sources with improved performance appear, combined with increased calculating power for signal analysis. As the interaction between target and electromagnetic field usually involves objects that can be described in only statistical terms, the outcome of the interaction itself will have to be described in the same terms. Thus, the statistics involved in the light/object interaction has to be understood in order to arrive at relevant parameters for the experiment. Likewise, the optimization of the measurement system will rely to a large extent on the proper understanding of the entire process. Needless to say, the full-scale setup can hardly be established before the performance has been contemplated, calling for simulation of the light/matter interaction. Therefore, fast and yet reliable simulation of this interaction is of crucial importance and is the subject of this study.

Various fields within optics call for such simulations, here focusing on simulation of 2D distributions, usually related to space variables. Within remote sensing, the phase disturbance between the receiver and the transmitter will due to phase disturbances in the path introduce intensity fluctuations, the statistical properties of which have to be understood in order to optimally retrieve the information. Thus, a 2D simulation of this phase perturbation scenario based on its power spectral density (PSD) and probability density function (PDF) is crucial [1]. Within microscopy, increased interest in light scattering from tissue in order to predict anomalies has appeared [2]. As biological tissue can best be described in statistical terms, the scattering parameters may reveal important changes within the tissue itself [3]. Recently, scattering of polarized light from biological tissue has shown promise for extracting new parameters, likewise calling for simulations [4]. Within sensing of dynamical properties of solid surfaces, knowledge about the scattering structure

1559-128X/12/100C77-07$15.00/0

becomes of importance, especially when the surface roughness does not exceed the optical wavelength, and/or the correlation length of the scattering structure becomes comparable with the illumination spot. Furthermore, the importance of a simulation increases when the PDF or the PSD depend on the direction, i.e., the structure is not isotropic. In case the surface roughness exceeds the wavelength and the illuminated area contains many correlation cells of the surface, the statistical parameters tend toward a Gaussian PDF, in which case the analysis is strongly simplified and thus has extensively been the subject of investigation. The statistical properties governing measurement of surface translation have previously been examined [5]. Of great importance here are situations where the signal consists of a sum of independent speckle contributions, in which case the statistical properties of the signal will have to be dealt with in details. An established method for measuring speckle displacement and thus surface movements is based on spatial filtering [6]. Here the spatial properties of the spatial distribution of the scattered intensity is important and strongly relies on the surface characteristics of the object. Statistics for glints from the ocean surface is a special application where knowledge about the scattering surface is imperative [7]. The distribution and strengths of the 2D distribution of reflective slopes here is responsible for the mean number of glints and the associated strength distribution for the glints. Unfortunately, the models for the surface statistics do not easily lead to analytical solutions, so one has to resort to simulations. Lately the issue of singularities in electromagnetic fields has become of increased interest due to the possibility of very precise localization of their position, which facilitates increased accuracy in determining speckle displacement and thus the dynamics of an object [8]. Here, as well, the need for simulation of the statistics of the structure becomes important. Finally, the distinction between scattering off stochastic surfaces having random and fractal characteristics has gained renewed interest due to the possibility of telling the difference between healthy and malignant tissue [9].

A method for simulation of homogeneous non-Gaussian stochastic vector fields has been published [10]. A random white Gaussian field is used as the seed, subsequently shaped into the desired PSD using an FFT algorithm. Finally, the derived representation is nonlinearly shaped in order to obtain the PDF. This calls for a series of iterative steps in order to arrive at reasonable results.

Methods for simulating 1D signals with a given PDF and PSD have previously been presented, starting with a Gaussian sample field followed by spectral shaping and then mapping this into a non-Gaussian PDF with a nonlinear and iterative process [11]. The iterative steps are here needed in order to arrive at a satisfactory result. A method specially developed in order to cope with PDFs where the inverse cumulative distribution function (CDF) is unavailable but reliance on digital simulation of the inversion process has been devised [12]. An alternative procedure has been developed, on the basis of the Markov theory, in which matching of the spectral density is accomplished by adjusting the drift coefficient alone, which is then followed by adjusting the diffusion coefficient to match the probability density [13].

Working with 2D signals, the amount of data needed for arriving at relevant results is usually large. Therefore, one may take advantage of symbolic programs like Mathematica and MatLab, which have analytical inversions of most CDFs, including some that were not available in [11]. Therefore, the present method will provide faster and usually sufficiently accurate results for random samples with given PSD and PDF. The method presented here for 2D signals with physically realizable PSDs is based on a previously presented method for 1D signals and will not require any iterations in order to arrive at results for engineering purposes [14]. Although this method does not conserve the PSD exactly, it yields highly accurate numerical results for a wide range of probability distributions and target PSDs that are sufficient for system simulation purposes. Thus by using modern fast computers one can even in 2D obtain fast and reliable results with this method. Apparently, this mapping technique is not well known to the optics community and it is our intent to indicate its usefulness and viability as a simulation tool for a wide range of practical applications. In any case, if more accurate results are desired, one can implement the iterative process outlined in [10] by properly expanding the method to encompass 2D signals. An iterative approach has been introduced [15] in which the Fourier transform method is used to create a Gaussian random process with the desired PSD, after which a memoryless nonlinear transformation is used to derive the PDF. The reason for this method and not the inverse CDF method is, according to the authors, that the CDF in many cases is not analytically convertible, as required. But by using built-in functions in analytical programs such as Mathematica and MatLab, one can benefit from the curve-fitting programs and thus achieve excellent results.

The straightforward noniterative inverse CDF method, as implemented here, is based on generating a white noise (noncolored) sample of a Gaussian distribution, which is easily obtained from many computer programs (e.g., Mathematica, Matlab, even Excel). In this paper and in [14] we consider only real stationary processes that are characterized by having autocorrelation functions with the property that their first and second derivatives evaluated at zero time and/or lag equals zero and is negative, respectively [16]. In particular, exponential decaying and exponential decaying cosine autocorrelation functions are not considered because their first and second derivatives evaluated at the origin are −1 and 1, respectively, and thus cannot be representative of real physical processes.

It is evident that it is impossible to check the accuracy of the resulting simulations for all possible PDFs and PSDs, and the interested user of this technique should use the method described here to see if this method is viable for any given case of interest. In this regard we note for an arbitrary PDF we presented in Appendix B of [14] a general rule of thumb to obtain the parameter range where a single (i.e., noniterative) application of the inverse CDF method yields satisfactory results. The same procedure can be employed for the 2D situation presented here. Outside this parameter range of applicability, the agreement between the simulated and target PSD degrades but does not significantly distort in shape. In any case, a slight discrepancy between the desired and the obtained simulation has to be weighed against the validity of the physical assumptions leading to the model.

In Section 2, we describe the method for creating a sample of a signal with a desired PDF and PSD, followed by a treatment and discussion for a series of examples, relevant within optics. These examples include the gamma distribution, the log-normal distribution, and the Rice–Nakagami distribution, relevant for treating integrated speckles, light propagation through optical turbulence, and speckles superimposed with a reference wave, respectively. Concluding remarks are given in Section 3.

2. Two-Dimensional Simulations of a Stochastic Process

In this section we extend the analysis in [14] and present a method by which 2D spatial spectrally colored non-Gaussian homogeneous stochastic fields can be generated, consistent with an arbitrary spatial PSD. Although for clarity of presentation we specialize to 2D fields (e.g., speckle intensity field distribution in an observation plane), the extension of the method presented here to three or more dimensions is straightforward. Consider an arbitrary stationary stochastic 2D random field $Z(x,y)$ characterized at each point in the $\{x,y\}$ plane by a given PDF $p_Z(z)$ [or equivalently by the corresponding CDF $F_Z(z)$]. As discussed and explicitly demonstrated in [14], for a single application of the inverse CDF transform method one obtains very good agreement for both the simulated samples of non-Gaussian probability distributions and the given PSD, as is the case for all the examples considered here.

In what follows, we denote random fields by uppercase letters and the values they assume at each point by lowercase letters, and p_Z and F_Z are referred to as the "target PDF" and "target CDF," respectively. Following the development in [14], we assume that a procedure is available for generating independent white noise samples of a random field $Z_1(x,y)$ (e.g., a Gaussian random field). Then the random variable at each point $\{x,y\}$

$$Z_0 = F_Z^{-1}(F_{Z_1}[z_1]) \tag{1}$$

where F_Z^{-1} is the inverse target CDF, has the distribution F_Z. Therefore, target distribution samples of Z can be generated from Z_1 transformed according to Eq. (1). In the following, for brevity in notation, we omit the subscripts on the distribution under consideration. As discussed in [1], the major advantage of this type of Monte Carlo simulation is that accurate results can be readily obtained in a timely manner for any random variable whose distribution function is known either analytically or numerically.

Here, as in [14], we use, via a single application of Eq. (1), a zero mean, unit variance colored (with a given PSD) Gaussian distribution as a "seed" to obtain a large number of independent samples of a given target distribution. For a large number of samples, this Gaussian seed produces corresponding sample values that have arbitrary means and variances, as implicitly contained in the inverse of the target CDF, with a corresponding (spatial) power spectrum that is a satisfactory approximation between the simulated and target PSDs that are sufficient for system simulation purposes. Thus, this method can be regarded as an accurate engineering approximation, which can be used for a wide range of practical applications. Here we use the Fourier transform spectral representation method applied for simulation purposes by Yamazaki and Shinozuka [17] and Shinozuka and Deodatis [18]. In this method, as used here, a discrete 2D Fourier transform of $N \times N$ independent zero mean, unit variance Gaussian distributed spatial sample values is preformed. Denote the spatial sample length in both the x and y coordinate by L and the corresponding sample spacing by l_S, respectively, where $L = Nl_S$. These white noise samples are then "colored" in the Fourier domain by multiplying each of the i-j-th spatial wavenumber components by $\sqrt{2S(K_{xi}, K_{yj})\Delta K}$, where S is the PSD of interest, K_{xi} and $K_{yj}$are the ith and jth spatial wavenumbers in the x and y directions, respectively, $\Delta K = K_U/N \times N$, and K_U represents an upper cutoff wavenumber beyond which the PSD may be assumed to be zero for either physical or mathematical reasons. Although the technique used here to obtain "colored" stochastic field samples is applicable to non-isotropic spatial power spectra (i.e., physical situations where the spatial field correlation depends on direction), we assume for simplicity that isotropic conditions are applicable, as they are for many physical situations (e.g., stellar scintillation, laser induced speckle). Consequently, here we assume that the PSD is a function of $\sqrt{K_x^2 + K_y^2}$ [19]. As an aid to the reader in making this article self-contained we explicitly present the various PDFs and PSDs illustrated here that were also used in [1].

As an example of the utility of the present method, we consider, as in [14], the continuous beta distribution with shape parameters α and β, whose mean and variance are given by$\alpha/(\alpha+\beta)$ and $\alpha\beta/[(\alpha+\beta)^2(1+\alpha+\beta)]$, respectively. The CDF and corresponding inverse CDF of the beta distribution are given by [20]

$$F(z) = \text{BetaRegularized}[z, \alpha, \beta], \quad \text{for } 0 \le z \le 1, \quad (2)$$

$$F^{-1}(z) = \text{InverseBetaRegularized}[z, \alpha, \beta], \quad \text{for } 0 \le z \le 1. \quad (3)$$

A beta distribution with shape parameter $\alpha = 4$, $\beta = 2$ is chosen here in order to consider a skewed distribution, and following Yamazaki and Shinozuka [17] we choose a Gaussian shaped target PSD of the form

$$S(K) = \frac{\sigma^2 l_C^2}{4\pi} \exp[-(K_x^2 + K_y^2) l_C^2/4], \quad (4)$$

where σ^2 is the variance and l_C is a measure of the spatial correlation length of the underlying process. Here and in what follows it is implicitly understood that the variance of the target distribution is identical to the variance obtained by integrating the PSD over all spatial wavenumbers. In Fig. 1 the beta stochastic field is shown as generated for the Gaussian shaped PSD with the number of data points equal to 10^4 ($N = 100$) and $l_C = 10 l_S$.

As another illustrative example, we apply the noniterative inverse CDF method to an example of a PDF and PSD regarding ocean wave surface heights, where the empirical model PDF is given by [21]

$$p(z) = \frac{2\phi^2(\kappa) z}{(1 - \kappa z)^3} \exp\left[-\phi^2(\kappa)\left(\frac{z}{1 - \kappa z}\right)^2\right], \quad \text{for } 0 \le z < 1/\kappa, \quad (5)$$

where $z = H/H_{\mathrm{rms}}$ is the normalized wave height, H is the wave height, H_{rms} is the root mean square wave height, $0 \le \kappa \le 1$ is a dimensionless parameter that controls the shape of the wave height distribution [for $\kappa = 0$ Eq. (5) is the Rayleigh distribution, and for $\kappa \to 1$ it becomes the Dirac Delta distribution], and $\phi(\kappa) = (1 - \kappa^{0.944})^{1.187}$. The corresponding CDF and inverse CDF are given by

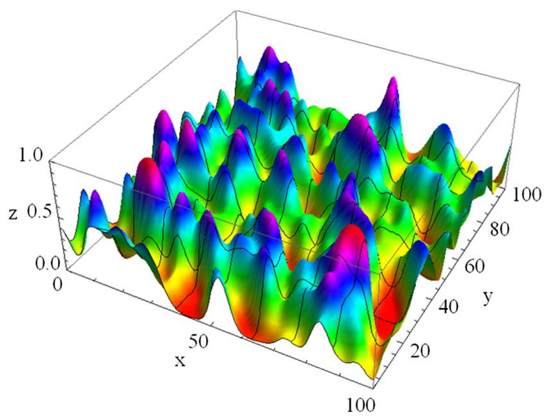

Fig. 1. (Color online) The beta stochastic field generated for the Gaussian shaped PSD with the number of data points equal to 10^4 ($N = 100$), and $l_C = 10 l_S$.

$$F(z) = 1 - \exp\left[-\phi^2(\kappa)\left(\frac{z}{1 - \kappa z}\right)^2\right], \quad \text{for } 0 \le z < 1/\kappa, \quad (6)$$

$$F^{-1}(z) = \frac{\phi(\kappa)\sqrt{-\log(1 - z)} + \kappa \log(1 - z)}{\phi^2(\kappa) + \kappa^2 \log(1 - z)}, \quad \text{for } 0 \le z \le 1. \quad (7)$$

The authors of [21] used a shape parameter $\kappa = 0.5$ and the Pierson Moskowitz PSD given by

$$S_{\mathrm{PM}}(K) = \frac{4\sigma^2}{K_N^5} \exp(-K_N^{-4}), \quad (8)$$

where $K_N = l_C \sqrt{K_x^2 + K_y^2}$ is the normalized spatial wavenumber, l_C is a measure of the spatial correlation length, and σ^2 is the variance of the process. Figure 2 shows an example of a resulting spatial field distribution section consisting of 10^4 sample points, and $l_C = 10 l_S$.

We next present illustrative examples based on the noniterative inverse CDF method of stochastic field distributions primarily of interest to the optics community. As indicated above, in what follows, it is implicitly understood that the variance corresponding to the target PDF is identical to the variance obtained by integrating the PSD over all wavenumbers.

A. Gamma Distribution

The gamma distribution has been used extensively in the literature to model the PDF of integrated speckle either from spatial or time averaging [22,23]. The CDF and corresponding inverse CDF are given by

$$F(z) = 1 - \frac{\Gamma(m, mz)}{\Gamma(m)}, \quad \text{for } z \ge 0, \quad (9)$$

$$F^{-1}(z) = Q^{-1}(m, 0, z), \quad \text{for } 0 \le z \le 1, \quad (10)$$

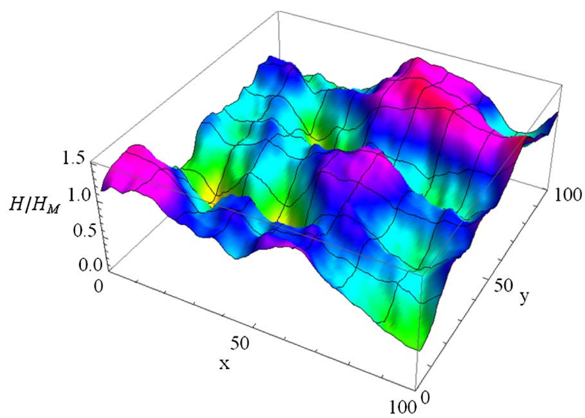

Fig. 2. (Color online) Ocean height field for a Pierson–Moskowitz PSD with an empirical model, Eq. (5), for the PDF, here for a resulting spatial field distribution section consisting of 10^4 sample points, and $l_C = 10 l_S$.

where for simplicity in notation we have normalized the (intensity) level, z, to its mean; $Q^{-1}(m, 0, z)$ is the inverse gamma regularized function; and $\Gamma(m, mz)$ is the incomplete gamma function [20]. The parameter m can be physically interpreted as the mean number of speckles contained within a collecting aperture [23]. Two correlation functions commonly appearing in measurements related to speckle phenomena are the Gaussian, given by Eq. (4), used in speckle correlation [5], and that obtained from laser reflection off of a rough circular surface of diameter D given by [22]

$$S(\upsilon) = \begin{cases} \left(\frac{2\sqrt{2}\lambda R}{\pi D}\right)^2 \left(\cos^{-1}(\upsilon l_C) - \upsilon l_C \sqrt{1-(\upsilon l_C)^2}\right), & \text{for } 0 \le \upsilon l_C \le 1 \\ 0 & \text{otherwise} \end{cases}, \tag{11}$$

where $\upsilon = \sqrt{\upsilon_x^2 + \upsilon_y^2}$ is the corresponding spatial frequency; $l_C = \lambda R/\pi D$ is a measure of the speckle size; λ is the optical wavelength; and R is the distance between the circular diffuse surface and the observation plane. Figures 3(a) and 3(b) show an example of a resulting fully developed speckle ($m = 1$) spatial intensity field distribution section consisting of a section 200×200 sample points, and $l_C = 10 l_S$ for the Gaussian and circular aperture PSD, respectively. Examination of these figures reveals that both PSDs produce qualitatively similar distributions, with the ratios of maximum/minimum values of 50.2 and 53.1 dB, respectively. To illustrate the effects of integrated speckle we plot in Fig. 4 the intensity field distribution for the PSD resulting from a Gaussian aperture and $m = 7.5$. The corresponding sample mean, variance, and ratio of maximum/minimum values are 1.04, 0.124, and 10.1 dB, respectively.

B. Log-Normal Distribution

The log-normal distribution for the irradiance distribution is applicable for laser propagation through the atmosphere under weak scintillation conditions [24]. As an illustrative example we consider the optical irradiance statistics associated with ground-based stellar observations at modest elevation angles. Under conditions where the log-intensity variance $\sigma_{\ln I}^2 \ll 1$, the log-normal CDF, and the corresponding inverse CDF can be expressed as

$$F(z) = \frac{1}{2}\left(1 + \mathrm{erf}\left[\frac{\log z + \sigma_{\ln I}^2/2}{\sqrt{2}\sigma_{\ln I}}\right]\right), \quad \text{for } z \ge 0, \tag{12}$$

$$F^{-1}(z) = \exp[z\sigma_{\ln I} - \sigma_{\ln I}^2/2], \quad \text{for } 0 \le z \le 1, \tag{13}$$

where z denotes the irradiance level normalized to its mean value. For weak scintillation conditions, Tatarskii has shown that the spatial log-intensity correlation coefficient and corresponding PSD are given by [25]

$$S(K) = \frac{2.577}{\omega^{8/3}}\left(1 - \frac{8\Gamma(17/6)}{11\Gamma(7/3)K^2}\,\mathrm{Im}[e^{i\omega^2}U(K)]\right), \tag{14}$$

where

$$U(K) = \frac{\pi}{\sin(\pi b)}\left(\frac{{}_1F_1(a; b; -iK^2)}{\Gamma(b)\Gamma(a-b+1)} - \frac{(-iK^2)^{1-b}\,{}_1F_1(a-b+1; 2-b; -iK^2)}{\Gamma(a)\Gamma(2-b)}\right). \tag{15}$$

"Im" denotes the imaginary part, $a = 1/2$, $b = -4/3$ and ${}_1F_1(\cdot)$ is the Kummer confluent hypergeometric

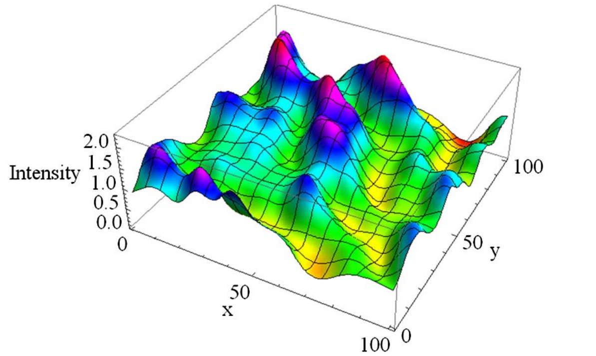

Fig. 4. (Color online) Integrated speckle field for the PSD resulting from a Gaussian aperture and $m = 7.5$.

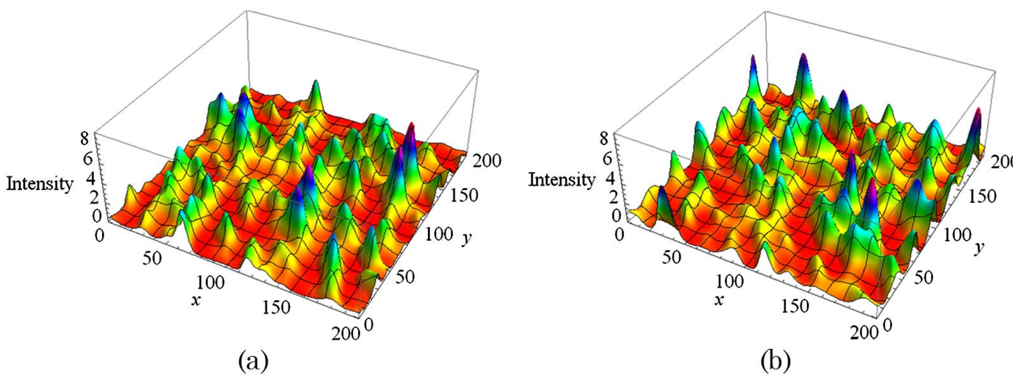

Fig. 3. (Color online) Example of a resulting fully developed speckle ($m = 1$) spatial intensity field distribution section consisting of a section 200×200 sample points, and $l_C = 10 l_S$ for the Gaussian (a) and circular aperture (b) PSD, respectively.

function. In Fig. 5 we plot the normalized intensity field distribution for the log-normal distribution for $\sigma^2_{\ln I} = 0.3$ for $l_C = 5l_S$.

C. Rice–Nakagami Distribution

As a final example, we illustrate the utility of obtaining a simulated stochastic field distribution whose corresponding CDF cannot be obtained analytically. We consider the Rice–Nakagami distribution [26]. The PDF and CDF of the Rice–Nakagami are given by

$$p(z) = 2z \exp[-(z^2 + C^2)] I_0(2zC), \quad \text{for } z \geq 0, \tag{16}$$

$$F(z) = \int_0^z 2\mu \exp[-(\mu^2 + C^2)] I_0(2\mu C) \mathrm{d}\mu, \quad \text{for } 0 \leq z \leq 1, \tag{17}$$

where $I_0(\cdot)$ is the modified Bessel function of first kind of order zero, C is a real constant, and both z and C are normalized to the "square root" of twice the variance of the underlying normal distribution [26]. In a variety of applications, the Rice–Nakagami distribution is used to model the intensity distribution in a speckle pattern that consists of a specular component and a diffuse scattered component [27]. In order to obtain a colored Rice–Nakagami sample distribution we proceed as in [14]. First, for a given value of C a tabulated set of data values in the form $\{F(z_i), z_i\}$ over a suitable range of z-values is obtained via numerical integration of Eq. (17). Next for the Rice–Nakagami distribution an accurate nonlinear fit of this "data set" to a model inverse CDF function of the form $F^{-1}_{\mathrm{RN}}(z) = az^n + a_1 z + a_3 z^3 + a_5 z^5 + b \log(1 - z)$ is made, where a, n, a_1, a_3, a_5, and b the model fit parameters to be determined. Finally, this analytic model is then used in Eq. (1) to obtain the suitable colored Rice–Nakagami sample distribution. We choose $C = 1$ to illustrate the efficacy of this method [28]. Figure 6 shows the excellent comparison of the inverse CDF (dotted points) obtained

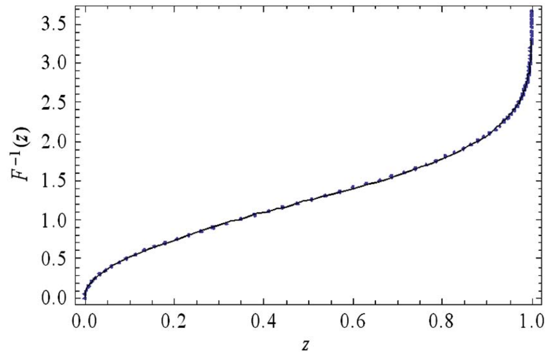

Fig. 6. (Color online) Comparison between the inverse CDF (dotted points) obtained numerically and the analytic model (solid curve) obtained via the least squares fit for the Rice–Nakagami distribution.

numerically to the analytic model (solid curve) obtained via the least squares fit. Figure 7 is the corresponding intensity field distribution for the PSD resulting from a circular aperture, 10^4 sample points, and $l_C = 10l_S$.

3. Concluding Remarks

A method for creating 2D distributions of signals with a desired PDF and PSD has been described. In contrast to previous methods, this method is noniterative and does not rely on autoregressive methods. This means that the creation of a given sample of reasonable size can be performed within a reasonable time, and thus a statistical reliable sample for analysis can be obtained. The method is based on establishing a 2D grid of Gaussian distributed random numbers, followed by spectral shaping with the desired spectrum. Finally, an inverse method is applied to the numbers in the grid, in order to achieve the desired PDF. It has previously been shown [14] that the autocorrelation function—and thus the PSD—in most cases are only slightly influenced by the inverse method. The inverse method relies on having an analytical expression for the inverse of the CDF of the desired PDF. Several examples relevant within optics have been treated, one of

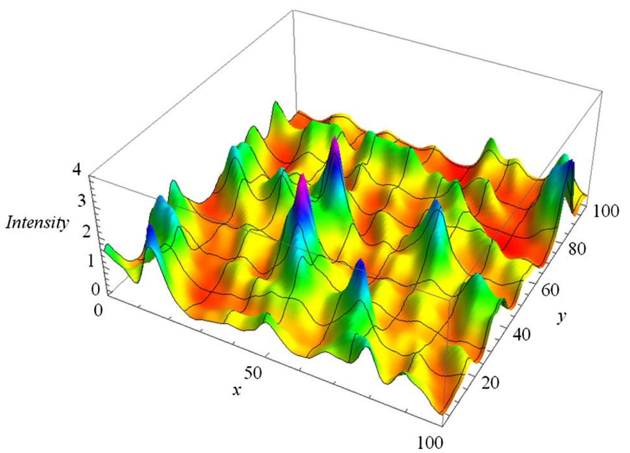

Fig. 5. (Color online) The log-normal normalized intensity field distribution for $\sigma^2_{\ln I} = 0.3$ for $l_C = 5l_S$.

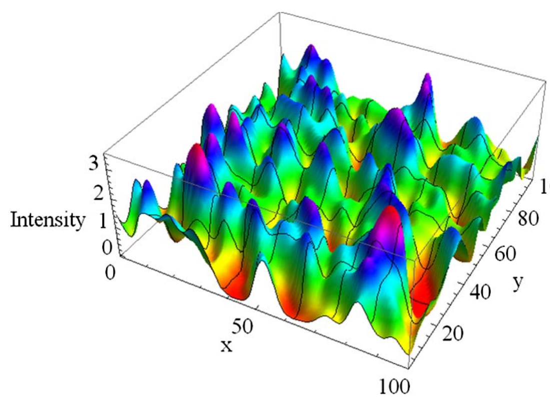

Fig. 7. (Color online) The intensity field distribution for the PSD resulting from a circular aperture, 10^4 sample points, and $l_C = 10l_S$ for the Rice–Nakagami distribution.

which (the Rice–Nakagami PDF) has no analytical expression for the inverse CDF. Here an excellent approximation has facilitated the inversion.

References and Notes

1. M. Borengasser, W. S. Hungate, S. William, and R. Watkins, *Hyperspectral Remote Sensing: Principles and Applications* (CRC Press, 2008).
2. T. Vo-Dinh, *Advanced Biomedical and Clinical Diagnostic Systems III* (SPIE, 2005).
3. R. Carminati, R. Elaloufi, and J.-J. Greffet, "Beyond the diffusing-wave spectroscopy model for the temporal fluctuations of scattered light," Phys. Rev. Lett. **92**, 213903 (2004).
4. S. Rehn, A. Planat-Chretien, M. Berger, J.-M. Dinten, C. Deumie, and A. da Silva, "Comparison of polarized light penetration depth in scattering media," Proc. SPIE **8088**, 80881I (2011).
5. U. Schnell, J. Piot, and R. Dändliker, "Detection of movement with laser speckle patterns: statistical properties," J. Opt. Soc. Am. A **15**, 207–216 (1998).
6. Y. Aizu and T. Asakura, *Spatial Filtering Velocimetry, Fundamentals and Applications*, Vol. **116** of Springer Series in Optical Science (Springer-Verlag, 2006).
7. V. N. Nosov and S. Yu. Pashin, "Influence of large-scale waves on the accuracy of sea surface parameters measurement by optical methods," Izv. Akad. Nauk SSSR, Fiz. Atmos. Okeana **24**, 53–58 (1988).
8. W. Wang, N. Ishii, S. G. Hanson, and M. Takeda, "Phase singularities in analytic signal of white-light speckle pattern with application to micro-displacement measurement," Opt. Commun. **248**, 59–68 (2005).
9. O. V. Angelsky, D. N. Burkovets, P. P. Maksimyak, and S. G. Hanson, "Applicability of the singular-optics concept for diagnostics of random and fractal rough surfaces," Appl. Opt. **42**, 4529–4540 (2003).
10. R. Popescu, G. Deodatis, and J. H. Prevost, "Simulation of homogeneous non-Gaussian stochastic vector fields," Prob. Eng. Mech. **13**, 1–13 (1988).
11. F. Yamazaki and M. Shinozuka, "Digital generation of non-Gaussian stochastic fields," J. Eng. Mech. **114**, 1183–1197 (1988).
12. S. S. Filho, J. C. Yacoub, and M. Candido Daoud, "Coloring non-Gaussian sequences," IEEE Trans. Signal Process. **56**, 5817–5822 (2008).
13. G. Q. Cai and Y. K. Lin, "Generation of non-Gaussian stationary stochastic processes," Phys. Rev. E **54**, 299–303 (1996).
14. H. T. Yura and S. G. Hanson, "Digital simulation of an arbitrary stochastic process by spectral representation," J. Opt. Soc. Am. A **28**, 675–685 (2011).
15. J. M. Nichols, C. C. Olson, J. V. Michalowitz, and F. Bucholtz, "A simple algorithm for generating spectrally colored non-Gaussian signals," Prob. Eng. Mech. **25**, 315–322 (2010).
16. P. Beckmann, *Probability in Communication Engineering*, (Harcourt, Brace & World, 1967), Section 6.6.
17. F. Yamazaki and M. Shinozuka, "Digital generation of non-Gaussian stochastic fields," J. Eng. Mech. Div., Am. Soc. Civ. Eng. **114**, 1183–1197 (1988).
18. M. Shinozuka and G. Deodatis, "Simulation of stochastic processes by spectral representation," Appl. Mech. Rev. **44**, 191–204 (1991).
19. We note under certain non-isotropic conditions [e.g., stratospheric turbulence; see, for example, C. Robert, J. M. Conan, V. Michau, J. B. Renard, C. Robert, and F. Dalaudier, "Retrieving parameters of the anisoptropic index fluctuations spectrum in the stratosphere from balloon-borne observations of scintillation," J. Opt. Soc. Am. A **25**, 379–393 (2008)] that the power spectra is a function of $\sqrt{K_x^2 + \eta^2 K_y^2}$, where the anisotropic parameter $\eta \geq 0$.
20. Wolfram, Mathematica, Version 7 (Cambridge University, 2008).
21. J. Mendez and S. Castanedo, "A probability distribution for depth-limited extreme wave heights in a sea state," Coastal Eng. **54**, 878–882 (2007).
22. J. W. Goodman, *Speckle Phenomena in Optics: Theory and Applications* (Roberts, 2006).
23. R. Barakat, "Level-crossing statistics of aperture averaged-integrated isotropic speckle," J. Opt. Soc. Am. A **5**, 1244–1247 (1988).
24. L. C. Andrews, R. L. Phillips, and C. Y. Hopen, *Laser Beam Scintillation with Applications* (SPIE, 2001), Chap. 2.
25. V. I. Tatarskii, *The Effects of the Turbulent Atmosphere on Wave Propagation* (Israel Program for Scientific Translations, 1971).
26. The CDF of the Rice–Nakagami distribution can be expressed in terms of a Marcum Q function, which are tabulated but not supported, to the best of our knowledge, by any commercial commuter programs such as Mathematica and Matlab.
27. J. W. Goodman, *Speckle Phenomena in Optics: Theory and Applications* (Roberts, 2006), Sec. 3.2.2.
28. For this case we obtain that the non linear least squares fit parameters are given by $n = -0.441$, $a = 1.24$, $a1 = 0.460$, $a3 = -0.516$, $a5 = 0.634$, and $b = -0.216$.